

Decoupling Identification with Closed-loop-controlled Elements for Two-link Arm with Elastic Joints

Junji Oaki ^{*,**} Shuichi Adachi ^{**}

^{*} Corporate Research and Development Center, Toshiba Corporation
Kawasaki, Japan (e-mail: junji.oaki@toshiba.co.jp).

^{**} Faculty of Science and Technology, Keio University
Yokohama, Japan (e-mail: adachi@appi.keio.ac.jp).

Abstract: The purpose of our study is to build a precise model by applying the technique of system identification for the model-based control of a nonlinear robot arm, taking joint-elasticity into consideration. We previously proposed a systematic identification method, called “decoupling identification”, for a “SCARA-type” planar two-link robot arm with elastic joints caused by the Harmonic-drive reduction gears. The proposed method serves as an extension of the conventional rigid-joint-model-based identification. The robot arm is treated as a serial two-link two-inertia system with nonlinearity. The decoupling identification method using link-accelerometer signals enables the serial two-link two-inertia system to be divided into two linear one-link two-inertia systems. The MATLAB’s commands for state-space model estimation are utilized in the proposed method. Physical parameters such as motor inertias, link inertias, joint-friction coefficients and joint-spring coefficients are estimated through the identified one-link two-inertia systems. This paper describes an accuracy evaluation of the identification method through experimental results using the two-link arm with “closed-loop-controlled elements”. The results show the method is applicable to a “PUMA-type” vertical robot arm under gravity.

Keywords: Robot arms; Nonlinear systems; Mechanical resonance; Frequency response; Multivariable systems; Closed-loop identification; Nonlinear optimization; MATLAB.

1. INTRODUCTION

The industrial robots with serial links, called SCARA (Selective Compliant Assembly Robot Arm) or PUMA (Programmable Universal Manipulation Arm), are widely used. Nowadays, the robots are required to be controlled with high acceleration and suppressed vibration. The dynamic model-based control considering the joint-elasticity of the robot (Ott (2008)) is necessary in order to satisfy this requirement. Although rigid-joint-model-based identification has been researched from a quarter-century ago (Khalil et al. (2002)), the field of elastic-joint-model-based identification is still in its infancy. Albu-Schäffer et al. (2001) showed a simple identification method for a 7dof elastic-joint robot using joint torque sensors, motor encoders, link encoders and motor brakes. However, coupled vibration effects caused by the elastic joints in the serial links are not considered.

The purpose of our study is to build a precise model by applying the technique of system identification for the model-based control of a nonlinear robot arm, taking joint-elasticity into consideration. We previously proposed a systematic identification method, called “decoupling identification”, for a “SCARA-type” planar two-link robot arm with elastic joints caused by the Harmonic-drive[®] reduction gears, shown in Fig.1 (Oaki et al. (2008)). The proposed method serves as an extension of the conventional rigid-joint-model-based identification.

The robot arm is treated as a serial two-link two-inertia system with nonlinearity. The decoupling identification method using link-accelerometer signals enables the serial two-link two-inertia system to be divided into two linear one-link two-inertia systems. The MATLAB[®]’s commands for state-space model estimation are utilized in the proposed method. Physical parameters such as motor inertias, link inertias, joint-friction coefficients and joint-spring coefficients are estimated through the identified one-link two-inertia systems. This is a gray-box approach.

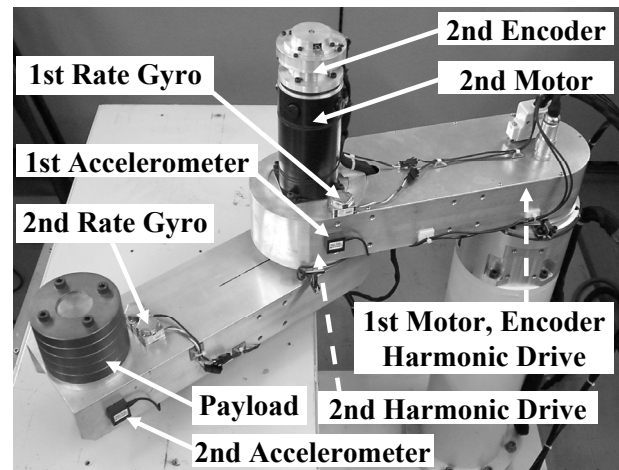


Fig. 1. Planar serial two-link robot arm with elastic joints.

In the procedure of the decoupling identification method, a pseudo random binary signal (PRBS) is applied to the 1st (or 2nd) joint by open-loop control as input data for identification while the 2nd (or 1st) joint is free because of no control. That is to say, the method is prepared as open-loop identification. However, in order to apply the method to a PUMA-type vertical two-link robot arm, it is necessary to maintain the link-posture under gravity by closed-loop control applied to the free joint.

In the followings, first, the previously proposed “decoupling identification” method (Oaki et al. (2008)) is described in detail. Next, the main purpose of this paper, an accuracy evaluation of the identification method through experimental results using the two-link arm with “closed-loop-controlled elements”.

2. TARGET SYSTEM

In this paper, a controlled object is the planar serial two-link robot arm with elastic joints shown in Fig. 1. A DC motor drives each joint with the Harmonic-drive gear that behaves as a linear spring element. The arm mechanism is similar in structure to the SCARA robot's 1st and 2nd links. This means that two one-link two-inertia systems are located in series. We call the mechanism a “serial two-link two-inertia system” (Oaki et al. (2008)). The drive systems for the 1st and 2nd joints have identical structures. However, the 2nd joint performs not only rotational motion but also translational motion. The coupled vibrational characteristics of the 2nd joint are more complicated than those of the 1st joint.

Payloads made of five brass disks (1kg per disk) are attached at the tip of the 2nd link. The payloads can be changed in the range of 5kg to 0kg. Each motor has a built-in rotary encoder for measuring the motor rotation angle. An accelerometer (bandwidth: 300 Hz) for measuring the link translational acceleration is mounted on each link. Angular acceleration of each link is computed by the coordinate transformation. Angular velocity of each link is computed by the sensor-fusion operation using the difference of the encoder signal with a low-pass filter and the integration of the angular acceleration signal with a high-pass filter, described below. A rate gyro (bandwidth: 5 Hz) mounted on each link is only used for testing an accuracy of the link-angular-velocity computation.

The link angular accelerations and velocities are utilized for computing the nonlinear interaction torques between two links. The link angular velocities in addition to the motor angular velocities are useful for improving identification accuracy. A real-time Linux PC is utilized for arm control and the data collection for identification.

3. DYNAMIC MODEL OF SERIAL TWO-LINK TWO-INERTIA SYSTEM

The dynamic model of the serial two-link two-inertia system (Ott (2008)) is given by

$$\begin{aligned} & \mathbf{M}_M \ddot{\boldsymbol{\theta}}_M + \mathbf{D}_M \dot{\boldsymbol{\theta}}_M + \mathbf{f}_M \text{sgn}(\dot{\boldsymbol{\theta}}_M) \\ &= \mathbf{E} \mathbf{u} - \mathbf{N}_G [\mathbf{K}_G (\mathbf{N}_G \boldsymbol{\theta}_M - \boldsymbol{\theta}_L) \\ & \quad + \mathbf{D}_G (\mathbf{N}_G \dot{\boldsymbol{\theta}}_M - \dot{\boldsymbol{\theta}}_L)] \end{aligned} \quad (1)$$

$$\begin{aligned} & \mathbf{M}_L(\boldsymbol{\theta}_L) \ddot{\boldsymbol{\theta}}_L + \mathbf{c}_L(\dot{\boldsymbol{\theta}}_L, \boldsymbol{\theta}_L) + \mathbf{D}_L \dot{\boldsymbol{\theta}}_L \\ &= \mathbf{K}_G (\mathbf{N}_G \boldsymbol{\theta}_M - \boldsymbol{\theta}_L) + \mathbf{D}_G (\mathbf{N}_G \dot{\boldsymbol{\theta}}_M - \dot{\boldsymbol{\theta}}_L) \end{aligned} \quad (2)$$

$\boldsymbol{\theta}_M = [\theta_{M1}, \theta_{M2}]^T$: motor rotation angle (1, 2: link number)

$\boldsymbol{\theta}_L = [\theta_{L1}, \theta_{L2}]^T$: link rotation angle

$\mathbf{M}_L(\boldsymbol{\theta}_L) \in R^{2 \times 2}$: link inertia matrix

$\mathbf{c}_L(\dot{\boldsymbol{\theta}}_L, \boldsymbol{\theta}_L) \in R^{2 \times 1}$: Coriolis and centrifugal force vector

$\mathbf{M}_M = \text{diag}(m_{M1}, m_{M2})$: motor-side inertia

$\mathbf{D}_M = \text{diag}(d_{M1}, d_{M2})$: motor-side viscous friction coefficient

$\mathbf{D}_L = \text{diag}(d_{L1}, d_{L2})$: link-side viscous friction coefficient

$\mathbf{K}_G = \text{diag}(k_{G1}, k_{G2})$: gear-spring coefficient

$\mathbf{D}_G = \text{diag}(d_{G1}, d_{G2})$: gear-dumping coefficient

$\mathbf{N}_G = \text{diag}(n_{G1}, n_{G2})$: gear-reduction ratio ($n_{G1}, n_{G2} \leq 1$)

$\mathbf{f}_M = [f_{M1}, f_{M2}]^T$: motor-side Coulomb friction torque

$\mathbf{E} = \text{diag}(e_1, e_2)$: torque / input-voltage coefficient

$\mathbf{u} = [u_1, u_2]^T$: input voltage (motor-current control reference).

The link inertia matrix is given by

$$\mathbf{M}_L(\boldsymbol{\theta}_L) = \begin{bmatrix} \alpha + \beta + 2\gamma \cos(\theta_{L2}) & \beta + \gamma \cos(\theta_{L2}) \\ \beta + \gamma \cos(\theta_{L2}) & \beta \end{bmatrix}, \quad (3)$$

where α, β , and γ are the base dynamic parameters (Khalil et al. (2002)) of the two-link robot arm. For convenience, $m_{L1} \equiv \alpha + \beta + 2\gamma$ is defined for the maximum value of the element (1, 1) in the link inertia matrix. Also, $m_{L2} \equiv \beta$ is defined for the constant value of the element (2, 2).

The Coriolis and centrifugal force vector is given by

$$\mathbf{c}_L(\dot{\boldsymbol{\theta}}_L, \boldsymbol{\theta}_L) = \begin{bmatrix} -\gamma(2\dot{\theta}_{L1}\dot{\theta}_{L2} + \dot{\theta}_{L2}^2) \sin(\theta_{L2}) \\ \gamma\dot{\theta}_{L1}^2 \sin(\theta_{L2}) \end{bmatrix}. \quad (4)$$

Since the torsional angles of the elastic joints are very small, the trigonometric functions $\cos(\theta_{L2})$ and $\sin(\theta_{L2})$ can be computed using the approximation $\theta_{L2} = n_{G2}\theta_{M2}$. The purpose of our study is to develop an accurate estimation method for the physical parameters that appear in (1) and (2). It is necessary to estimate β and γ previously for the proposed method. Therefore, the rigid-joint model is required using the approximation $\boldsymbol{\theta}_M = \mathbf{N}_G^{-1}\boldsymbol{\theta}_L$ in (1) and (2) as

$$\begin{aligned} & \mathbf{M}(\boldsymbol{\theta}_L) \ddot{\boldsymbol{\theta}}_L + \mathbf{c}_L(\dot{\boldsymbol{\theta}}_L, \boldsymbol{\theta}_L) + \mathbf{D} \dot{\boldsymbol{\theta}}_L \\ & \quad + \mathbf{N}_G^{-1} \mathbf{f}_M \text{sgn}(\dot{\boldsymbol{\theta}}_M) = \mathbf{N}_G^{-1} \mathbf{E} \mathbf{u} \end{aligned} \quad (5)$$

$$\mathbf{M}(\boldsymbol{\theta}_L) = \begin{bmatrix} \alpha + \beta + 2\gamma \cos(\theta_{L2}) + m_{M1}/n_{G1}^2 & \beta + \gamma \cos(\theta_{L2}) \\ \beta + \gamma \cos(\theta_{L2}) & \beta + m_{M2}/n_{G2}^2 \end{bmatrix} \quad (6)$$

$$\mathbf{D} = \text{diag}(d_{L1} + d_{M1}/n_{G1}^2, d_{L2} + d_{M2}/n_{G2}^2), \quad (7)$$

where $\mathbf{M}(\boldsymbol{\theta}_L)$ and \mathbf{D} are the inertia matrix and viscous-friction coefficient matrix respectively. The parameters in (5) can be estimated by the conventional rigid-joint-model-based identification method (Khalil et al. (2002)).

4. SIGNAL PROCESSING FOR MEASURING LINK-SIDE STATE VARIABLES

Each of the link angular accelerations is computed by the coordinate transformation of the link translational accelerations using the accelerometer signals as

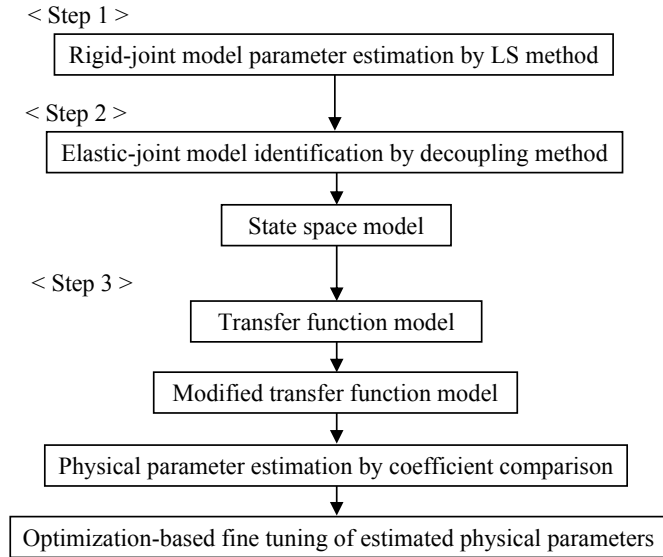


Fig. 2. Outline of the proposed identification method.

$$\ddot{\theta}_{L1} = \frac{a_1}{l_{a1}} \quad (8)$$

$$\ddot{\theta}_{L2} = \frac{a_2}{l_{a2}} - \frac{a_1}{l_{a1}} - \frac{a_1}{l_{a2}} \cos(n_{G2}\theta_{M2}) - \frac{l_{a1}}{l_{a2}} \ddot{\theta}_{L1}^2 \sin(n_{G2}\theta_{M2}) \quad (9)$$

where a_1, a_2 : link angular acceleration (1, 2: link number)
 l_{a1}, l_{a2} : mounting distance of accelerometer from each joint.

Each of the link angular velocities is computed by the sensor fusion operation using the difference of the encoder signal with a low-pass filter $G_L(s) = 1/(1 + T_V s)$ and the integration of the angular acceleration signal with a high-pass filter $G_H(s) = 1 - G_L(s)$ as

$$\dot{\theta}_{Li} = \frac{1}{1 + T_V s} (\dot{\theta}_{Mi} + T_V \ddot{\theta}_{Li}) \quad (i = 1, 2) \quad (10)$$

where T_V is a time constant for low-pass and high-pass filters.

5. DECOUPLING IDENTIFICATION WITH CLOSED-LOOP-CONTROLLED ELEMENTS

The previously proposed decoupling identification method (Oaki et al. (2008)) enables the serial two-link two-inertia system (1) and (2) to be divided into two linear one-link two-inertia systems. The method consists of the three steps shown in Fig. 2. The first step is the physical parameter estimation for the rigid-joint model. The second step is the state-space model estimation for each of the links based on the elastic-joint model. The third step is the physical parameter estimation for the elastic-joint model via two single-input single-output transfer functions converted from the state-space models. In this section, the procedure of the decoupling identification with "closed-loop-controlled elements" is introduced.

5.1 Physical parameter estimation for rigid-joint model

It is necessary to estimate β and γ in (5) previously for the proposed method. The conventional rigid-joint-model-based identification using the least-squares method (Khalil

et al. (2002)) can be applied to estimate the parameters in (5) with arbitrary motion data of the two-link robot arm. The data are low-pass-filtered for suppressing unmodeled-dynamics effects. The nonlinear interaction torques between two links are computable using the estimated $\hat{\beta}$ and $\hat{\gamma}$ and the link angular accelerations and velocities. This fact plays an important role in the proposed decoupling identification method. The estimated Coulomb friction torque should be removed from the motor input data for the state-space model estimation in the next subsection.

5.2 State-space model estimation for elastic-joint model

The proposed decoupling identification method enables the serial two-link two-inertia system (1) and (2) to be divided into two linear one-link two-inertia systems. Using (1) and (2), the state-space model expression for the 1st joint (Oaki et al. (2008)) is obtained as

$$\dot{\mathbf{x}}_1 = \mathbf{A}_1 \mathbf{x}_1 + \mathbf{B}_1 \begin{bmatrix} u_1 \\ \tau_1 \end{bmatrix}, \quad \mathbf{A}_1 \in R^{4 \times 4}, \quad \mathbf{B}_1 \in R^{4 \times 2} \quad (11)$$

$$\mathbf{y}_1 = \mathbf{C}_1 \mathbf{x}_1, \quad \mathbf{C}_1 \in R^{2 \times 4} \quad (12)$$

$$\mathbf{x}_1 \equiv [\theta_{M1}, \theta_{L1}, \dot{\theta}_{M1}, \dot{\theta}_{L1}]^T$$

$$\mathbf{y}_1 \equiv [\dot{\theta}_{M1}, \dot{\theta}_{L1}]^T$$

$$\tau_1 = -(\hat{\beta} + \hat{\gamma} \cos(\theta_{L2})) \ddot{\theta}_{L2} + \hat{\gamma} (2\dot{\theta}_{L1} \dot{\theta}_{L2} + \dot{\theta}_{L2}^2) \sin(\theta_{L2}), \quad (13)$$

where τ_1 is the nonlinear interaction torque from the 2nd link, computed using the link angular accelerations and velocities. The MATLAB's subspace-based "pem" or "n4sid" command (Ljung (2007)) is applicable to estimate the state-space model (11) and (12). The estimated model has two inputs, two outputs and four state variables. In this case, the motor input u_1 , where a PRBS is applied, and the computed torque τ_1 are employed as inputs for linearizing and decoupling in the multi-input identification. Furthermore, the link and motor angular velocity are employed as outputs for improving accuracy in the multi-output identification.

It is required that the element (1,1) in (3) is constant during the motion for the linear estimation commands. It is also required for τ_1 to have "frequency richness condition" for accurate identification. Therefore, it is necessary to investigate the element (1,1) in (3), and the power spectral density of τ_1 using experimental data. It is the same deriving procedure for the 2nd joint using (1) and (2). The nonlinear interaction torque from the 1st link can be computed using the link angular accelerations and velocities as

$$\tau_2 = -(\hat{\beta} + \hat{\gamma} \cos(\theta_{L2})) \ddot{\theta}_{L1} - \hat{\gamma} \dot{\theta}_{L1}^2 \sin(\theta_{L2}). \quad (14)$$

5.3 Physical parameter estimation for elastic-joint model

Four single-input single-output transfer functions are obtained by converting from the state-space model (11) and (12) for the 1st joint as

$$\dot{\theta}_{M1}(s) = G_{11}(s) u_1 + G_{12}(s) \tau_1 \quad (15)$$

$$\dot{\theta}_{L1}(s) = G_{21}(s) u_1 + G_{22}(s) \tau_1. \quad (16)$$

The transfer function $G_{11}(s)$ from motor input u_1 to motor angular velocity $\dot{\theta}_{M1}$ is expressed using the six physical parameters as

$$G_{11}(s) = \frac{b_0 + b_1s + b_2s^2}{a_0 + a_1s + a_2s^2 + a_3s^3} \quad (17)$$

where $a_0 = d_{M1} + n_{G1}^2 d_{L1}$
 $a_1 = m_{M1} + n_{G1}^2 m_{L1}$
 $\quad + (n_{G1}^2 d_{G1} d_{L1} + d_{M1} d_{L1} + d_{M1} d_{G1})/k_{G1}$
 $a_2 = (m_{M1} d_{L1} + m_{M1} d_{G1}$
 $\quad + m_{L1} d_{M1} + n_{G1}^2 m_{L1} d_{G1})/k_{G1}$
 $a_3 = m_{M1} m_{L1}/k_{G1}$
 $b_0 = 1, b_1 = (d_{L1} + d_{G1})/k_{G1}, b_2 = m_{L1}/k_{G1}.$

A set of six simultaneous equations is obtained by the coefficient comparison using (17) and the transfer function conversion from the estimated state-space model above. The six physical parameters are obtained by solving the simultaneous equations.

However, when the sampling rate for identification is selected to be fast for estimating the vibrational characteristics caused by the elastic joints, the results in the low-frequency region may be inaccurate. In order to modify the low-frequency region of the estimated transfer function (17), the first-order lag element of the denominator is replaced using the estimated physical parameters for the rigid-joint model above as

$$G_{11}(s) = \frac{b_0 + b_1s + b_2s^2}{(c_0 + c_1s)(d_0 + d_1s + d_2s^2)} \quad (18)$$

where $c_0 = d_{M1} + n_{G1}^2 d_{L1}$, $c_1 = m_{M1} + n_{G1}^2 m_{L1}$, $d_0 = 1$. This approximation is valid when the cut-off frequency of the first-order lag element is low enough compared with the frequency of the vibrational characteristics. The six physical parameters for the 1st joint are now obtained by solving (17) and (18). It is the same deriving procedure for the 2nd joint.

Furthermore, fine tuning of the estimated physical parameters is performed using closed-loop simulations with the nonlinear least-squares optimization (Mathworks (2007)). The parameter-search ranges are selected to be small (25%) to ensure the convergence. All physical parameters are simultaneously optimized except the coulomb friction torque because of its nonlinearity.

5.4 Dynamic model with closed-loop-controlled elements

In the procedure of the decoupling identification method with "closed-loop-controlled elements", a PRBS is applied to the 1st (or 2nd) joint by open-loop control as input data for identification while the 2nd (or 1st) joint is locked by closed-loop control using a PI velocity servo as

$$u_i = k_{IVi} \int (\dot{\theta}_{MRi} - \dot{\theta}_{Mi}) dt - k_{PVi} \dot{\theta}_{Mi} \\ = -k_{IVi} \theta_{Mi} - k_{PVi} \dot{\theta}_{Mi} \quad (i = 1, \text{ or } 2) \quad (19)$$

where

- $\dot{\theta}_{MRi}$: motor angular velocity reference (= 0)
- $\dot{\theta}_{Mi}$: motor angular velocity
- k_{IVi} : integral feedback control parameter
- k_{PVi} : proportional feedback control parameter
- u_i : input voltage (motor-current control reference).

The integral control enables to generate a torque for maintaining the link-posture under gravity. Therefore, this method is also applicable to a PUMA-type vertical two-link robot arm. It can be considered that (17) is as a partial state-feedback. When the decoupling identification method using link-accelerometer signals ideally works for the 1st (or 2nd) joint, it should be not related to whether the 2nd (or 1st) joint is closed-loop controlled or not. However, the subspace identification method (n4sid) is not suitable to closed-loop identification (Ljung (2007)). In the next section, identification experiments using the two-link arm are conducted to verify the closed-loop effects.

6. EXPERIMENTAL RESULTS AND DISCUSSIONS

The proposed decoupling identification method was verified through experiments performed using the SCARA-type planar two-link robot arm with 5 kg payload (Fig. 1). The physical parameter estimation for the rigid-joint model was previously performed.

6.1 Open-loop identification

A PRBS was applied to the 1st joint by open-loop control as input data for identification while the 2nd joint was free because of no control. The sampling time for input and output data was set to 0.025 ms. Since the PRBS (period: 1023) was produced at 1 ms intervals, data collection continued for 1.023 s. The sampling time 1 ms was changed to 2 ms using decimation. The PRBS amplitude was set to 10.0 V (maximum). These identification conditions were determined by some trial and error. Fig. 3 shows the PRBS input data (first 0.3 s of 1.023 s). Fig. 4 shows nonlinear interaction torque data and its power spectral density. Although the spectral density is somewhat bumpy, it is satisfactory in practice as another input data for multi-input identification. It was checked the cosine of the 2nd link angle was changing with value of 0.999 or more, during the 1st link motion for identification. Therefore, the element (1, 1) in (3) is regarded as constant.

Two-input two-output state-space model can be estimated using the input and output data by the MATLAB's "pem" command (Ljung (2007)). In Fig. 5, the solid lines show the estimated frequency response from motor input u_1 to motor angular velocity $\dot{\theta}_{M1}$. A typical vibrational characteristics of a one-link two-inertia system such as (17) are shown. In Fig. 5, the lines show the frequency response after the modification using (18). Fig. 6 shows the optimization-based fine tuning of the estimated physical parameters using the 1st-link angular-velocity step responses of the real arm and simulation. In Fig. 5, the chain lines show the optimized frequency response after the nonlinear least-squares optimization (Mathworks (2007)).

Also, Fig. 7 shows the typical vibrational characteristics of the one-link two-inertia system for the 2nd link. This means that coupling effects between the 1st and 2nd links are decoupled by the proposed method. The estimated values of the physical parameters via (17) are introduced in the reference (Oaki et al. (2008)).

In Fig. 8, the solid lines estimated by the proposed decoupling identification method, using the computed torques and motor inputs, show the typical characteristics of the

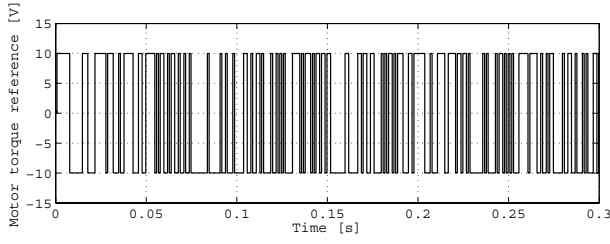


Fig. 3. Pseudo random binary signal (PRBS) input data for 1st link identification (first 0.3 s of 1.023 s).

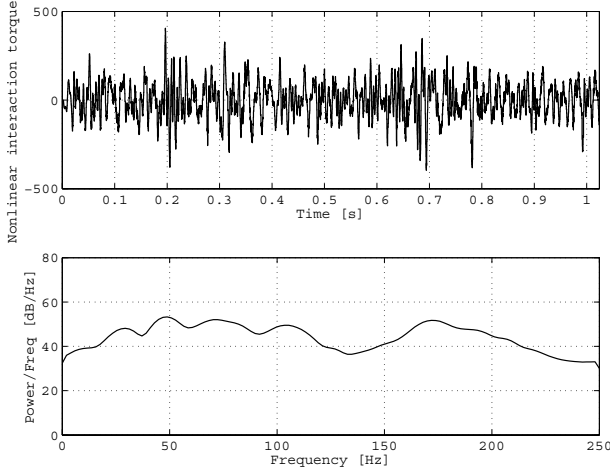


Fig. 4. Nonlinear interaction torque data for 1st link identification and its power spectral density, where 2nd link is free.

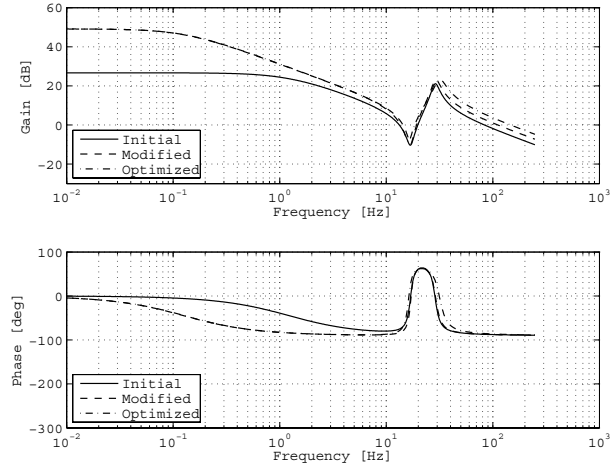


Fig. 5. Modification and optimization of initial estimated frequency responses for 1st link from motor input u_1 to motor angular velocity θ_{M1} .

one-link two-inertia systems. The dashed lines estimated by the method that utilizes only motor inputs cannot express the characteristics because of the interaction torques. These phenomena are remarkable at the 2nd link.

6.2 Closed-loop identification

A PRBS was applied to the 1st (2nd) joint by open-loop control as input data for identification while the 2nd (1st) joint was locked by closed-loop control using the PI velocity servo. Fig.9 shows power spectral density of

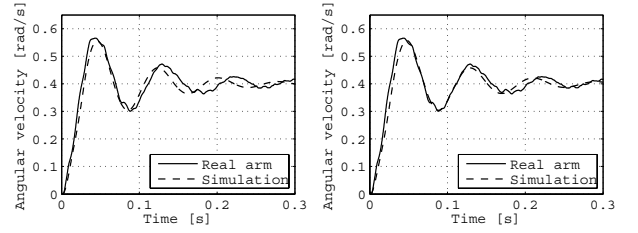


Fig. 6. Optimization-based fine tuning of estimated physical parameters using 1st link angular velocity step responses. Left: Before optimization. Right: After optimization.

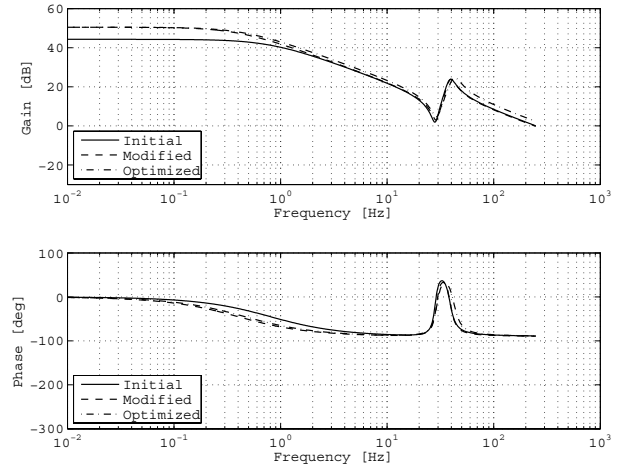


Fig. 7. Modification and optimization of initial estimated frequency responses for 2nd link from motor input u_2 to motor angular velocity $\dot{\theta}_{M2}$.

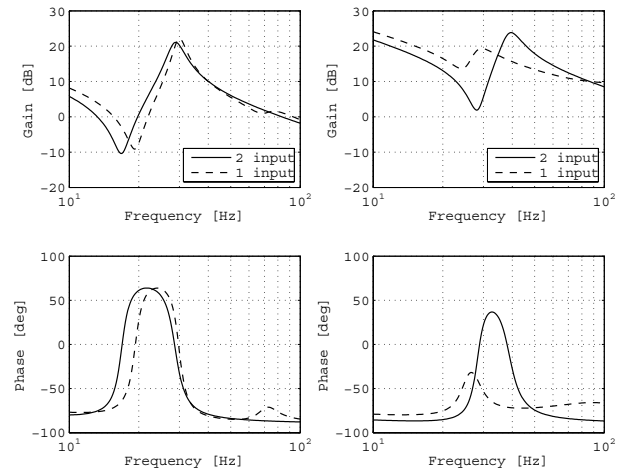


Fig. 8. Effective examples for decoupling identification from motor input to motor angular velocity. Left: 1st link. Right: 2nd link.

nonlinear interaction torque data for the 1st link identification, where the 2nd link is closed-loop controlled. Fig. 10 shows closed-loop effects against estimated frequency responses from motor input to motor angular velocity. Although the spectral density in Fig.9 is small in the low-frequency region compared with Fig.4, the left-hand figures in Fig.10(a) show the proposed method also works as closed-loop identification using the “pem” command. As opposed to it, the left-hand figures in Fig.10(b) show

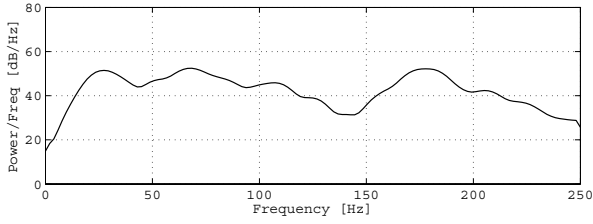


Fig. 9. Power spectral density of nonlinear interaction torque data for 1st link identification, where 2nd link is closed-loop controlled.

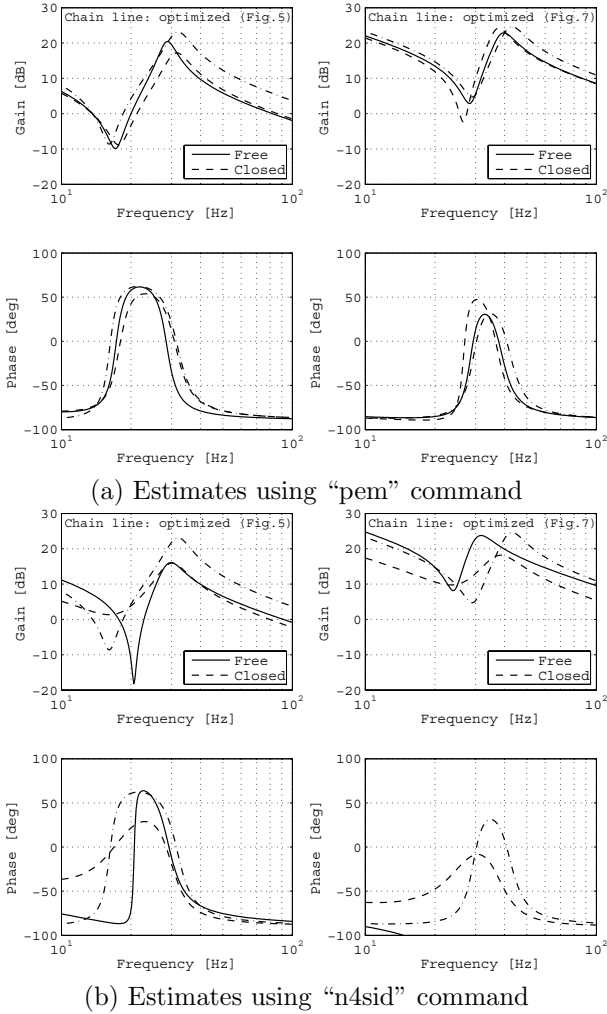


Fig. 10. Closed-loop effects against estimated frequency responses from motor input to motor angular velocity. Left: 1st link, where 2nd link is free or closed-loop controlled. Right: 2nd link, where 1st link is free or closed-loop controlled.

inaccurate results using the “n4sid” command. The right-hand figures in Figs.10(a) and (b) show similar results obtained for the 2nd link. Small (about 10%) errors in Figs.10(a) between the open-loop and closed-loop results can be recovered by the optimization-based fine tuning. The “pem” command is powerful because of the iterative prediction-error minimization based on the initial state-space model estimated using the “n4sid” command.

Fig. 11 shows cross-correlation functions between motor-input and residuals from motor-angular-velocity for the

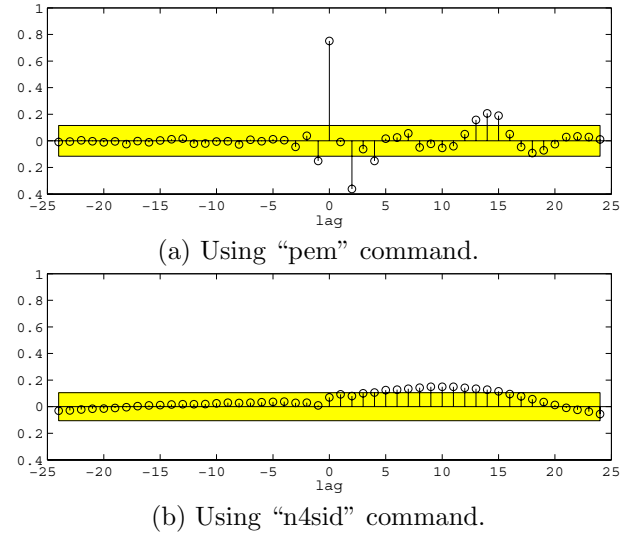


Fig. 11. Cross-correlation functions between motor-input and residuals from motor-angular-velocity for 2nd link, using “pem” or “n4sid” command, where 1st link is closed-loop controlled.

2nd link, using “pem” or “n4sid” command, where the 1st link is closed-loop controlled. The cross-correlations are little in Fig. 11(a). However, the cross-correlation is remarkable in Fig. 11(b). This means the subspace method “n4sid” based on the correlation absence of residuals is not suitable for closed-loop identification.

7. CONCLUSION

Experimental results using a SCARA-type planar two-link robot arm with elastic reduction gears show an accuracy of the proposed “decoupling identification” method. The precise model is obtained by applying the technique of system identification for the model-based control of a nonlinear robot arm, taking joint-elasticity into consideration. Although the method was prepared as open-loop identification, it was verified that the method also worked as closed-loop identification in this paper. Therefore, it is applicable to a PUMA-type vertical two-link robot arm which needs to maintain the link-posture under gravity.

REFERENCES

- A.Albu-Schäffer and G.Hirzinger. Parameter identification and passivity based joint control for a 7dof torque controlled light weight robot. *Proc. IEEE International Conference on Robotics and Automation*, pages 1087–1093, 2001.
- W.Khalil and E.Dombre. Modeling, Identification & Control of Robots. *Kogan Page Science*, 2002.
- L.Ljung. System Identification Toolbox for Use with MATLAB (Version 7.0). *The MathWorks*, 2007.
- The MathWorks. Optimization Toolbox for Use with MATLAB (Version 3.1.1). *The MathWorks*, 2007.
- J.Oaki and S.Adachi. Decoupling Identification and Physical Parameter Estimation for Serial Two-link Two-inertia System. *IEEJ Trans. IA*, Vol.128, No.5, pages 669–677, 2008 (in Japanese).
- C.Ott. Cartesian Impedance Control of Redundant and Flexible-Joint Robots. *Springer*, 2008.